# Influence of bath temperature and deposition time on hardness and magnetisation of electrodeposited Nickel Manganese Tungsten thin films

P. Kirthika [a], N.Thangaraj [* ab], P.Anitha [b]
[a] *Department of Physics, Velalar College of Engineering and Technology, Erode-12, Tamilnadu, India*
[b] *Department of Physics, Vellalar College for Women, Erode-12, Tamilnadu, India*

The Nickel Manganese Tungsten (Ni-Mn-W) thin films were prepared at different temperature and time of deposition on copper substrate. The crystal structure and morphology of deposits were analysed by X-ray diffraction (XRD) and scanning electron microscopy (SEM). The XRD revealed that the structure of Ni-Mn-W thin films with have an average grain size of about 28 nm for 45°C. The elemental analysis of Ni-Mn-W thin films were obtained by energy dispersive X-ray spectroscopy (EDAX). The magnetic properties of electrodeposited Ni-Mn-W thin films were obtained by vibrating sample magnetometer (VSM). The magnetic parameters of Ni-Mn-W films such as coercivity and saturation magnetization were decreased with increasing of grain size. The hardness of the films was studies by Vicker Hardness tester through diamond intender method.

(Received December 17, 2022; Accepted April 13, 2023)

*Keywords*: Electrodeposition, Ni-Mn-W, Hardness, Bath temperature

## 1. Introduction

Electrochemical supercapacitors (ESs) are becoming attractive as an energy storage device because they possess high power density, exhibit excellent reversibility, and have a very long cycle life. Carbon and transition metal oxides have been used for electrode materials of ESs. Carbon-based systems are thought to function as double –layer capacitors due to their high specific surface areas (about 2000 $m^2g^{-1}$). On the contrary, transition metal oxides (e.g. $RuO_2$, NiO, $CoO_x$, $MnO_2$, etc.) shows charge storage mechanisms based on pseudo capacitance.

The electrodeposition of semiconductors, metals and alloys has established an extensive utilize in the fabrication of micro electro mechanical system (MEMS) for the past decades. Ni and its high strength alloys employ more useful materials for MEMS application due to their vast usage in the form of mechanical and magnetic elements such as motors, precision gears, latches, flexure spring arms, high density recording media, a magnetic shield, high performance transformer cores and magnetic actuators [1]. Electrodeposition is simple, rapid and inexpensive method for preparing nano structured metal and alloy as thin films [2-4]. Electrodeposited Ni-Mn thin film posses high strength, good ductility and low stress used in microsystems and in probe spring applications [5,6]. The parameters used to control the process of deposition are pH, current density, bath temperature and complexing agent, etc [7-11]. In maximum investigations, Nickel Manganese alloys were electrodeposited from sulfamate and sulfate baths and very few from the bath containing chloride. Fathi et al. reported that the percentage of Mn content presents in the film increases with increasing current density. Moreover the effectiveness of cathode has enhanced by chloride ions and films were deposited even at low voltages due to the high conductivity of chloride bath [12,13]. The Ni-Mn alloy is an intellectual combination to investigate further in their abundant inimitable properties viz, the contradictory type of magnetic alignment in their fundamental state is one among them. The ferromagnetic nickel and paramagnetic manganese come together to produce Ni-Mn alloys with attractive magnetic properties [14]. Babanov et al.

* Corresponding author: knt_raj@yahoo.co.in
https://doi.org/10.15251/JOR.2023.192.231

reported that $Ni_{75}Mn_{25}$ shows paramagnetic behavior at room temperature and $Ni_{80}Mn_{20}$ shows ferromagnetic behavior [15].

Magnetic nanoparticles have attracted a lot of interest and research attention due to their potential application in a variety of fields. The complex magnetic behavior exhibited by nanoparticles is governed by many factors, including their size, composition, shape, morphology, and shell-core structure [16]. The increased surface to volume ratio and tailored structure in nanoparticles introduces many size dependent phenomena which may be used to optimize the physical and chemical properties. Sequence of phase transformation and magnetic properties may be effectively controlled by adjusting the particle size and atomic packing. Nanoscale magnetic materials are good candidates for magnetic refrigeration due to a presence of a large magnetocaloric effect (MCE) in the superparamagnetic system [17-19].

In this present study, structural, morphological, hardness and magnetic behavior of Ni-Mn-W films at different temperature were studied.

## 2. Experimental Details

A copper substrate of size 2 x 7 cm is used as cathode and nickel plate is used as anode. Both the electrodes were subjected to cleaning effect. The cathode is washed with 0.01N dilute sulphuric acid, followed by acetone wash and then with distilled water, where as Nickel plate is washed with acetone and then with hot double distilled water. Before subjecting to deposition the cathode plate is masked such that 2 x 5 cm alone is exposed for deposition.

Electrodepositon was carried out on the cleaned substrates at constant current density. Analytical grade chemicals were used in the experiment. The solution is taken in a beaker and the electrodes are fixed to obtain estimated coating area. A constant current density of $3mA/cm^2$ is applied through power supply.

Ni-Mn-W thin films were cathodically deposited using aqueous solutions of 0.1 M $NiCl_2.6H_2O$, 0.1 M of $MnCl_2.H_2O$ and 0.05M of $Na_2WO_4$ and maintaining the pH value in between 4 and 5 using concentrated $H_2SO_4$ acid. The bath temperature is varied to 35, 45 and $55^0C$ whereas the deposition time is optimized to 15, 30 and 45 minutes.

Structural studies of the Ni-Mn-W films were carried out using XRD. The morphology of the Ni-Mn-W thin films is studied with the aid of Scanning Electron Microscope (SEM). The chemical composition of the deposits was obtained by energy dispersive X-ray spectroscopy (EDAX). Magnetic properties of Ni-Mn-W thin films has been studied with vibrating sample magnetometer (VSM).

## 3. Results and discussion

### 3.1. Structural properties

The X-ray diffraction pattern of Ni-Mn-W thin films under different temperatures of 35, 45 and 55ºC is shown in Fig.1. From XRD patterns, it is clear that the deposited film is polycrystalline in nature with corresponding 2θ values are of 31.6, 34.7, 43.07, 44.4, 51.8, 67.4, and 74.4, respectively. Furthermore, the increase in temperature 35 °C to 55 °C, the intensity of peak and sharpness of the peaks increases. The crystallite size of Ni-Mn-W thin films were evaluated using equation 1.

$$D = \frac{0.94\lambda}{\beta \cos\theta} \tag{1}$$

where, $D$ is the grain size of crystallite, $\lambda$ is the wavelength of X-rays, $\beta$ is the broadening of diffraction line measured at half its maximum intensity in radians and $\theta$ is the angle of diffraction. The dislocation density and microstrain were calculated using the following equations 2 and 3;

$$\delta = \frac{1}{D^2} \tag{2}$$

$$\varepsilon = \frac{\beta \cos\theta}{4} \tag{3}$$

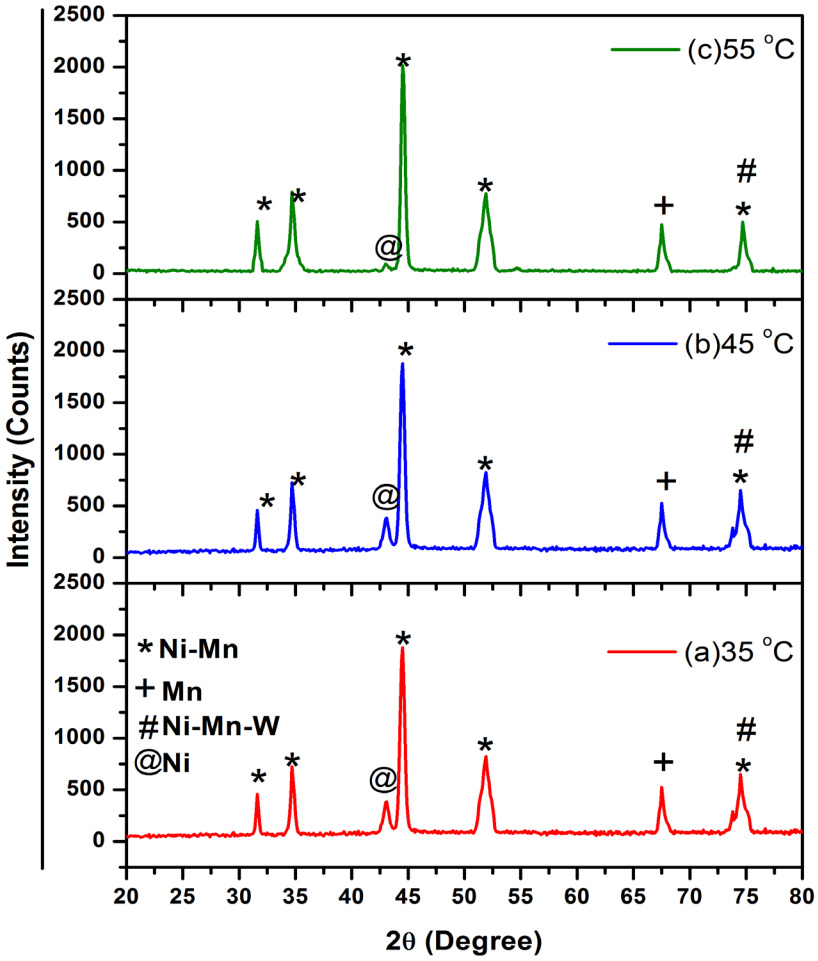


*Fig. 1. XRD pattern of Ni-Mn-W thin films were deposited at different bath temperatures (a) 35°C (b) 45°C and (c) 55°C*

The variation of crystallite size with bath temperature of Ni-Mn-W thin films are listed in Table 1. From Table 1, it is observed that the average crystallite size increases with temperature increase up to 45 °C and attains a maximum of ~30 nm. For sample with temperature 45°C, the minimum values for dislocation density and microstrain (Table 1) are obtained. The Ni-Mn-W thin films with lower microstrain and dislocation density may be included in impurities of tungsten.

*Table 1. The structural parameters of electrodeposited Ni-Mn-W thin films*

| Temperature (°C) | 2 Theta (degree) | d-spacing (Å) | FWHM (dθ) | Crystallite Size (nm) | Dislocation Density ($10^{15}$lin/m$^2$) | Micro Strain ($10^4$ lin$^{-2}$m$^{-4}$) |
|---|---|---|---|---|---|---|
| 35 | 31.6292 | 2.828 | 0.295 | 29.22 | 0.1170 | 12.38 |
| | 34.7433 | 2.582 | 0.295 | 29.46 | 1.1519 | 12.28 |
| | 43.0711 | 2.100 | 0.492 | 18.12 | 3.0438 | 19.96 |
| | 44.4905 | 2.036 | 0.393 | 22.80 | 1.9228 | 15.87 |
| | 51.8801 | 1.762 | 0.492 | 18.74 | 2.8447 | 19.30 |
| | 67.4923 | 1.387 | 0.393 | 25.38 | 1.5518 | 14.25 |
| | 74.4993 | 1.272 | 0.480 | 21.71 | 2.1215 | 16.67 |
| 45 | 31.5970 | 2.831 | 0.393 | 23.90 | 2.0845 | 16.52 |
| | 34.7431 | 2.582 | 0.295 | 34.44 | 1.1535 | 12.29 |
| | 43.0019 | 2.103 | 0.295 | 30.20 | 1.2963 | 14.98 |
| | 44.5354 | 2.034 | 0.492 | 30.21 | 2.2127 | 12.86 |
| | 51.8801 | 1.762 | 0.492 | 18.74 | 2.8447 | 14.30 |
| | 67.4833 | 1.387 | 0.393 | 25.34 | 1.5568 | 14.28 |
| | 74.6890 | 1.269 | 0.480 | 21.73 | 2.1162 | 13.65 |
| 55 | 31.6551 | 2.826 | 0.393 | 21.90 | 2.0839 | 16.52 |
| | 34.7430 | 2.582 | 0.295 | 38.44 | 1.1535 | 12.29 |
| | 43.3209 | 2.088 | 0.393 | 25.67 | 1.0446 | 15.96 |
| | 44.7324 | 2.025 | 0.492 | 18.23 | 3.0084 | 18.85 |
| | 51.8801 | 1.762 | 0.393 | 23.43 | 1.4206 | 15.44 |
| | 67.4993 | 1.387 | 0.393 | 25.34 | 1.2565 | 12.27 |
| | 74.6912 | 1.269 | 0.480 | 21.73 | 2.4461 | 12.66 |

### 3.2 Morphological analysis of Ni-Mn-W thin films

The morphology of Ni-Mn-W thin films was observed with scanning electron microscopy (SEM) and a sample image is shown in Fig. 2. The Ni-Mn-W films are obtained with micro cracks due to the internal stress. At a low current density, the surface is bright and smooth. The average sizes of synthesized Ni-Mn-W thin films were observed to be 23, 25 and 28 nm, in good agreement with crystallite size estimated from XRD data using well-known Debye-Scherrer relation. Further, increases in temperature up to 45ºC, with slightly increase in crystallite size and found to be 28 nm are observed from Fig. 2b. It is seen from Fig. 2c, the grains are uniform, tiny well boundary grains and found to be 25 nm. When the bath temperature increases from 35 ºC to 45ºC, the number of nuclei increases and the nuclei grow over the whole surface area of the substrate with uniform grains. The grain size became smaller with increase of bath temperature up to 45ºC. This is mainly due to the increase of migration ability of atoms and molecules on the surface during the growth at higher bath temperature.

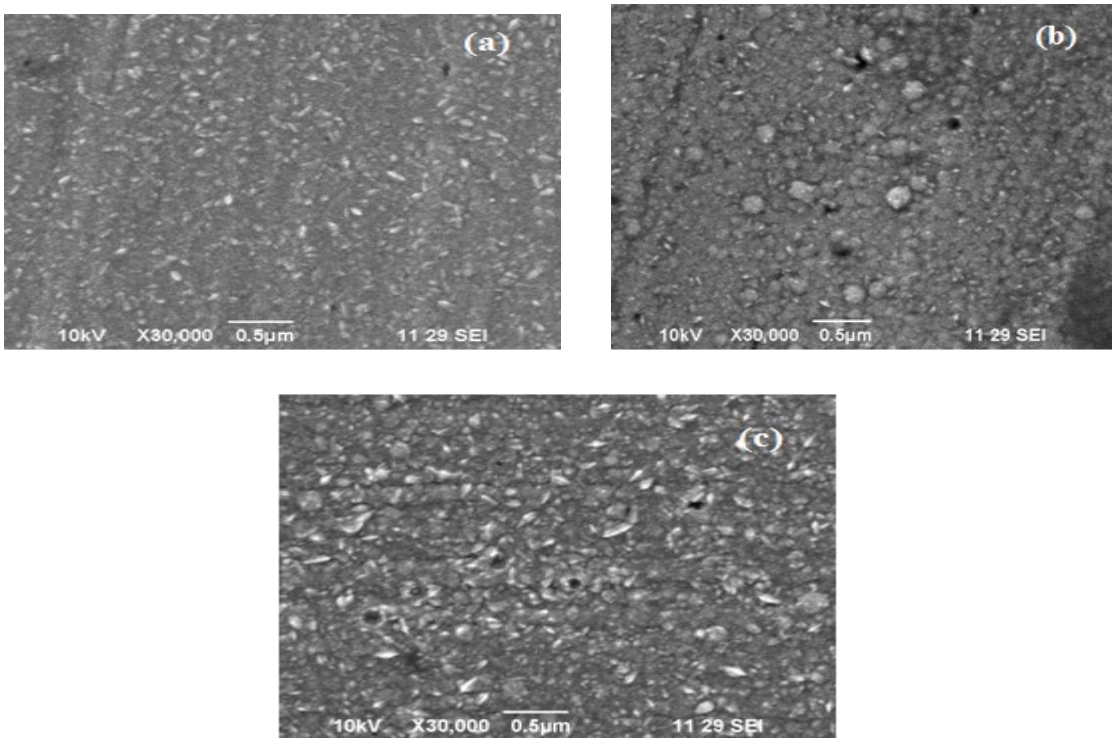


*Fig. 2. SEM images of Ni-Mn-W thin films were deposited at different bath temperatures (a) 35°C (b) 45°C and (c) 55°C*

### 3.3 Compositional analysis of Ni-Mn-W thin films

The presence of elemental composition of electrodeposited Ni-Mn-W thin films was confirmed by the Energy dispersive X-ray analysis.

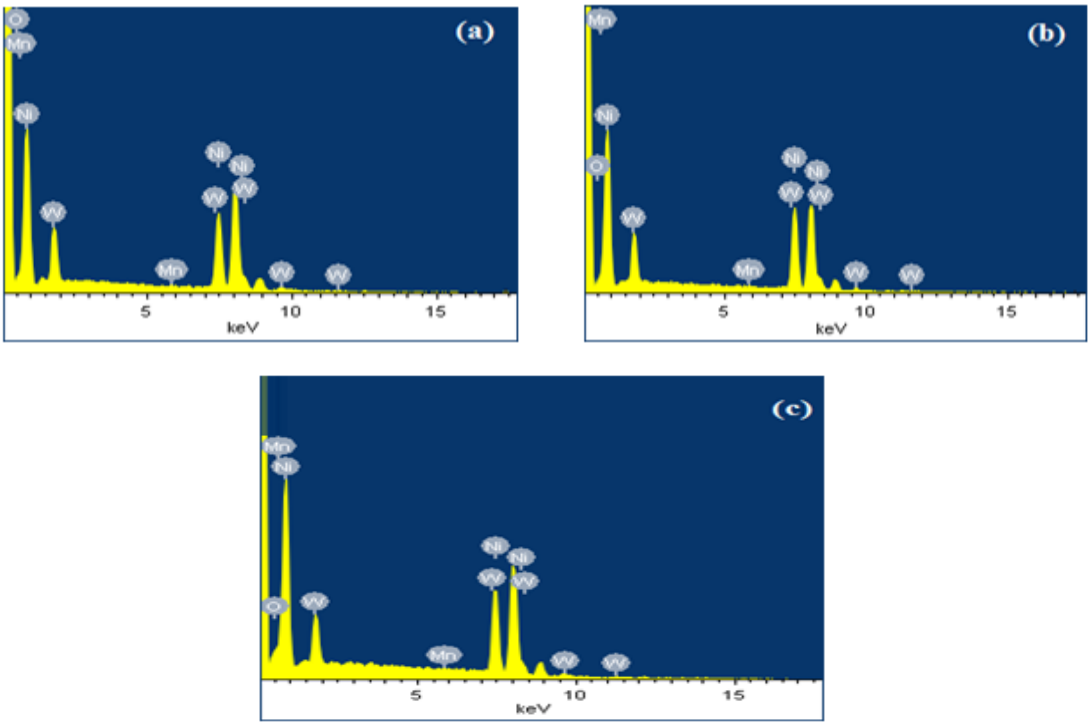


*Fig. 3. EDAX images of Ni-Mn-W thin films were deposited at different bath temperatures (a) 35°C (b) 45°C and (c) 55°C*

The samples were prepared at 35ºC, 45ºC and 55ºC is shown in Fig. 3. These spectra show that the expected elements exist in the solid films. It is observed that in Fig.3, initially the nickel content of the thin film increases progressively with the increases in bath temperature at 45ºC while decrease in Mn atomic percentage. Further, increase in temperature at 55ºC and stoichimetric of Ni-Mn-W thin films are observed.

### 3.4 Magnetic behavior of Ni-Mn-W thin films

The magnetic behaviour of electrodeposited Ni-Mn-W thin films were prepared at different bath temperatures 35ºC, 45ºC and 55ºC with various time of deposition 15, 30, and 45 min are shown in Fig. 4. Fig. 4a shows the magnetic behaviour of Ni-Mn-W thin film at room temperature. It is evident that the deposited film is paramagnetic in nature at room temperature. However, with an increase in time, the M-H loops of the films exhibit the nonlinear behavior which indicates ferromagnetic behavior. Development of ferromagnetism in the films can be attributed to the increase in the degree of crystalinity of the processed films as a function of time.

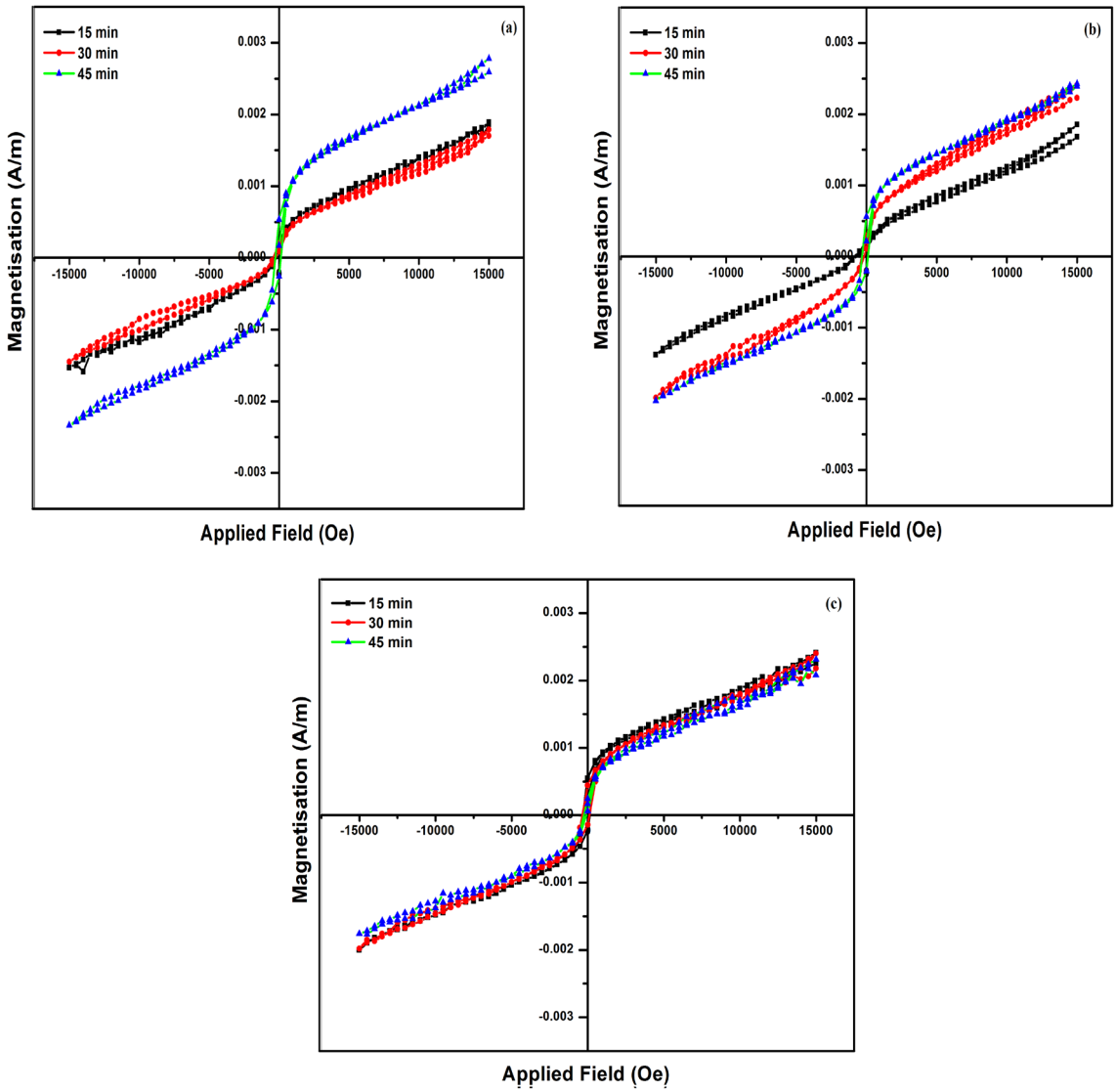


*Fig. 4. The magnetic hysteresis loops of electrodeposited Ni-Mn-W thin films at different bath temperatures (a) 35ºC (b) 45ºC and (c) 55ºC*

The coercivity of magnetic samples has a striking dependence on their grain size. As the grain size decreases, the coercivity increases to maximum and then decreases. The change in

coercivity is attributed to its change from the multidomain nature to single-domain superparamagnetic state by further decrease in grain size results in an unstable state where spin fluctuations dominates. Hence in the multi domain region, the coercivity decreases as the particle diameter increases. Below the critical diameter, where magnetization changes by spin rotation, the coercivity decrease is attributed to thermal effects. The variation of magnetization, Retentivity and coercivity are listed in Table 2.

*Table 2. The magnetic parameters of electrodeposited Ni-Mn-W thin films.*

| Bath temperature (°C) | Deposition time (min) | Magnetization x $10^{-3}$ emu | Retentivity x $10^{-3}$ emu | Coercivity (Oe) |
|---|---|---|---|---|
| 35 | 15 | 2.2013 | 0.38415 | 232.21 |
| | 35 | 2.1875 | 0.29277 | 214.73 |
| | 45 | 2.0403 | 0.09187 | 82.718 |
| 45 | 15 | 1.6171 | 0.05779 | 82.054 |
| | 35 | 1.7400 | 0.06589 | 82.392 |
| | 45 | 2.5611 | 0.39530 | 199.94 |
| 55 | 15 | 1.6178 | 0.03379 | 72.620 |
| | 35 | 2.1956 | 0.09310 | 75.291 |
| | 45 | 2.2285 | 0.38331 | 211.07 |

### 3.5 Mechanical properties of Ni-Mn-W thin films

Hardness of the sample was measured by using Vickers Hardness Number. Vickers Hardness measurements of electrodeposited Ni-Mn-W thin films at different bath temperatures and various load at 25 g, 50g, 100 g, 200g and 300 g are shown in Fig. 5.

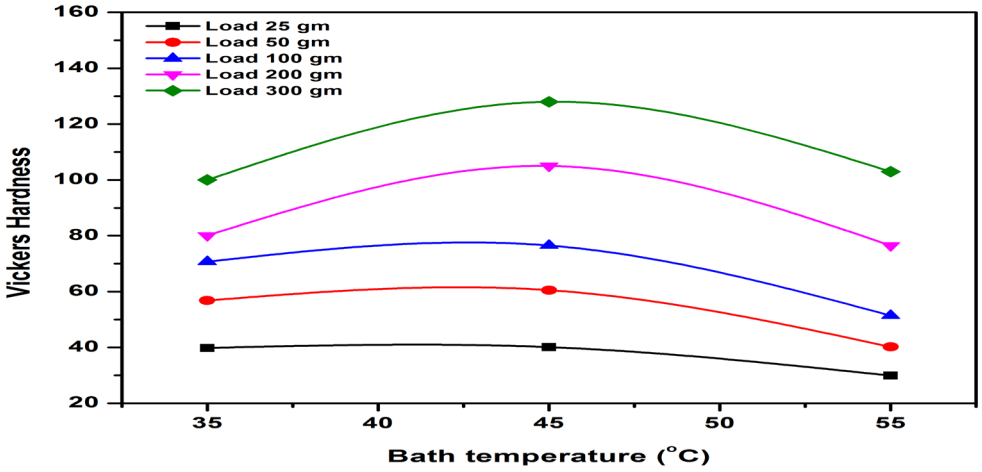


*Fig. 5. Vickers Hardness measurements of electrodeposited Ni-Mn-W thin films at different bath temperatures*

It is seen from Fig. 5, the hardness of the thin films were found to be increased with increase in bath temperature upto 45°C. It is due to the reduction of grain size and strain.

## 4. Conclusions

The structural, morphological, magnetic and mechanical properties of Ni-Mn-W thin films were investigated at different bath temperature. X-ray diffraction patterns confirmed the presence of polycrystalline in nature with relative intensities of the peaks obtained from the profiles match well with those calculated for the FCC structure of Ni-Mn-W thin films. The grain size was found to be about 23, 28, and 25 for Ni-Mn-W thin films deposits with bath temperatures 35, 45 and 55ºC respectively. SEM analysis showed a formation of tiny size of Ni-Mn-W nanoparticles with an average size of 23, 25, and 28 nm in close agreement with crystallite size estimation from XRD. EDAX results shows that stoichiometric films of good quality are obtained at a bath temperature of 45 ºC. The effects of bath temperature and time on the magnetic properties revealed a significant improvement in the magnetic properties of the Ni-Mn-W nanoparticles. Magnetization and coercivity decreased with increase in particle size. Hysteresis first decreased by reducing the size and then increased for the smallest sample. Thus we have shown that nanoparticles as compared to their bulk counterpart have an enhanced magnetization with less hysteresis which is especially important in the magnetic refrigeration technology to become commercially viable.

## Acknowledgements

The authors express their heartfelt thanks to IIT, Chennai for magnetic studies.

## References

[1] M. W. Losey, J. J. Kelly, Comprehensive Microsyst. **271** (2008). http://dx.doi.org/10.1016/B978-044452190-3.00010-0
[2] F. Stephen, L. Rossi, C. Nasi, N. Ferrari, M. V. Ponpandian, V. Ananth, J. Ravichandran, Appl. Phys. **103**, 053511, 1 (2008). https://doi.org/10.1063/1.2844211
[3] P. Kirthika, N. Thangaraj, Dig. J. Nanomat. Bio struct. **16(3)**, 855 (2021).
[4] T. Aruna Christy, N. Thangaraj, Dig. J. Nanomat. Bio struct. **16(3)**, 847 (2021).
[5] S. H. Goods, J. J. Kelly, N. Y. C. Yang, Technol. **10**, 498 (2004). https://doi.org/10.1007/s00542-004-0381-8
[6] B. Tunaboylu, Mater. Lett. **70**, 51 (2012). https://doi.org/10.1016/j.matlet.2011.11.089
[7] D. Sasikumar, N. Thangaraj, S. Ganesan, K. Tamilarasan, Chalcogenide Lett. **9**, 11 (2012).
[8] N. Thangaraj, K. Tamilarasan, D. Sasikumar, Dig. J. Nanomat. Bio struct. **9(1)**, 27 (2014).
[9] O. S. Agboola, Int. J. Phys. Sci. **7**, 349 (2012).
[10] X. Su, C. Qiang, Bull. Mater. Sci. **35**, 183 (2012). https://doi.org/10.1007/s12034-012-0284-8
[11] W. N. R. Abdullah, K. M. Hyie, N. A Resale, W. T. Chong, J. Adv. Mat. Res. **576**, 565 (2012). https://doi.org/10.4028/www.scientific.net/AMR.576.565
[12] R. Fathi, S. Sanjabi, C. Appl. Phys. 12, 89 (2012).https://doi.org/10.1016/j.cap.2011.04.047
[13] R. Fathi, S. Sanjabi, N. Bayat, Mater. Lett. **66**, 346 (2012). https://doi.org/10.1016/j.matlet.2011.08.102
[14] C. B. Zimm, M. B. Stearns, J. Magn. Magn. Mater. **50**, 223 (1985). https://doi.org/10.1016/0304-8853(85)90186-6
[15] Yu. A. Babanov, V. P. Pilyugin, T. Miyanaga, A. M. Patselov, E. G. Chernyshev, A. V. Ryazhkin, T. Ogasavara, Journal of Surface Investigation. X-ray, Synchrotron and Neutron Techniques, **1**, 3, 359 (2007)
[16] A. Kolhatkar, A. Jamison, D. Litvinov, R. Willson, T. Lee, Int. J. Mol. Sci. **14**, 15977–16009 (2013). https://doi.org/10.3390/ijms140815977
[17] A. Horrocks, B. Kandola, G. Milenes, A. Sitpalan, R. Hadimani, Polymer Degradation and Stability **97(12)**, 2511–2523 (2012). https://doi.org/10.1016/j.polymdegradstab.2012.07.003
[18] S. P. Gubin, Yu A. Koksharov, G. B. Khomutov, and G. Y. Yurkov, Russian Chemical Reviews **74(6)**, 489–520 (2005).
[19] R. D. McMichael, R. D. Shull, L. J. Swartzendruber, L. H. Bennett, R. E. Watson, J. Magn. Magn. Mater. **111**, 29–33 (1992).https://doi.org/10.1016/0304-8853(92)91049-Y